Phyton-
International Journal of
Experimental Botany

Tech Science Press

DOI: 10.32604/phyton.2024.048192

ARTICLE

Three New Hydroxytetradecenals from *Amomum tsao-ko* with Protein Tyrosine Phosphatase 1B and Glycogen Phosphorylase Inhibitory Activity

Xiaolu Qin[1,3], Xinyu Li[1,3], Yi Yang[2], Mei Huang[2], Shengli Wu[1], Pianchou Gongpan[1], Lianzhang Wu[2], Juncai He[2] and Changan Geng[1,3,*]

[1]State Key Laboratory of Phytochemistry and Plant Resources in West China, Kunming Institute of Botany, Chinese Academy of Sciences, Kunming, 650201, China

[2]Nujiang Green Spice Industry Research Institute, Lushui, 673100, China

[3]University of Chinese Academy of Sciences, Beijing, 100049, China

[*]Corresponding Author: Changan Geng. Email: gengchangan@mail.kib.ac.cn

Received: 30 November 2023 Accepted: 27 March 2024 Published: 28 May 2024

ABSTRACT

The fruits of *Amomum tsao-ko* (Cao-Guo) were documented in Chinese Pharmacopoeia for the treatment of abdominal pain, vomiting, and plague. In our previous study, a series of diarylheptanes and flavonoids with α-glucosidase and protein tyrosine phosphatase 1B (PTP1B) inhibitory activity have been reported from the middle-polarity part of *A. tsao-ko*, whereas the antidiabetic potency of the low-polarity constituents is still unclear. In this study, three new hydroxytetradecenals, (2*E*, 4*E*, 8*Z*, 11*Z*)-6*R*-hydroxytetradeca-2,4,8,11-tetraenal (**1**), (2*E*, 4*E*, 8*Z*)-6*R*-hydroxytetradeca-2,4,8-trienal (**2**) and (2*E*, 4*E*)-6*R*-hydroxytetradeca-2,4-dienal (**3**) were obtained from the volatile oils of *A. tsao-ko*. The structures of compounds **1–3** were determined using spectroscopic data involving 1D and 2D nuclear magnetic resonance (NMR), high-resolution mass spectra (HRMS), and specific rotation ($[\alpha]_D$). Their hypoglycemic activity was evaluated against glycogen phosphorylase (GPa) and PTP1B. Compounds **1** and **2** displayed moderate activity against PTP1B with inhibition rates of 33.8%–50.3% at 100 and 200 μM. Moreover, compound **1** exhibited an obvious inhibitory effect on GPa (IC_{50} = 31.7 μM), whereas compound **2** was inactive. This study demonstrates hydroxytetradecenals as the characteristic components of *A. tsao-ko* with therapeutic potential in diabetes.

KEYWORDS

Cao-Guo; PTP1B and GPa inhibitors; diabetes mellitus; volatile oils

1 Introduction

Diabetes mellitus (DM) is a chronic metabolic disease characterized by fasting or postprandial hyperglycemia, which results from insulin deficiency and insulin resistance [1]. DM can lead to serious complications such as heart attack, diabetic kidney disease, cerebrovascular disease, and neuropathy [2]. About 537 million people are suffering from DM all over the world, of which type 2 diabetes (T2DM) occupies more than 90% of the cases [3]. Medicines are the main treatment strategy for T2DM and can be sketchily classified into oral and injection drugs according to their administration methods. Currently, several types of oral hypoglycemic drugs are available in the market, but their application is limited by

This work is licensed under a Creative Commons Attribution 4.0 International License, which permits unrestricted use, distribution, and reproduction in any medium, provided the original work is properly cited.

the inevitable side effects and drug resistance [4]. Medicinal herbs are always considered to be important sources of new drugs, especially the plants used for both medicines and foods [5–8].

Amomum tsao-ko belonging to the Zingiberaceae family has a widespread distribution across Yunnan, Guangxi, and Guizhou Provinces of China [9]. Its dried fruits (Tsaoko Fructus, Cao-Guo in Chinese) are a well-known traditional Chinese medicine documented in Chinese Pharmacopoeia for the treatment of abdominal pain, vomiting, and plague. As a "medicine-food homology" material, Cao-Guo is widely consumed as a spice in the indigenous diets of East and Southeast Asian countries [10]. The major constituents of *A. tsao-ko* are essential oils, terpenoids, diarylheptanoids, flavonoids, phenols, amino acids, and saccharides [11]. Previous investigation manifested that *A. tsao-ko* had antidiabetic [12], cytotoxic [13], neuroprotective, anti-inflammatory [14], antioxidant [15], antimicrobial and antiviral effects [16,17]. Yu et al. reported that *A. tsao-ko* showed efficacy in promoting insulin secretion and increasing insulin sensitivity by regulating digestive enzymes, as well as reducing the plasma-free fatty acid concentration to improve insulin resistance [18,19]. In our latest study, a variety of diarylheptanoids and flavonoids with α-glucosidase and PTP1B inhibitory effects were isolated from the ethyl acetate part of Cao-Guo, indicating the antidiabetic potency of the phenols [20–24].

Volatile oils are another type of constituent in Cao-Guo, which should be no less than 1.4% in the crude drugs according to the latest edition of Chinese Pharmacopoeia. Presently, more than one hundred constituents have been detected in its volatile oils, which are mainly 1,8-cineole, *α*-pinene, *β*-pinene, lemonol, *α*-citral, *α*-terpineol and *α*-phellandrene [25,26]. However, most of the volatile oils were only tentatively characterized by LCMS analysis, and their exact structures and biological activity were little studied.

To fully understand the antidiabetic potency of Cao-Guo, its petroleum ether soluble part was further investigated. As a result, three new hydroxytetradecenals were purified and unambiguously characterized by substantial spectroscopic data (Fig. 1). Their antidiabetic activity was evaluated against two diabetes-related enzymes, namely PTP1B and GPa. Their separation, structural analysis, and antidiabetic effects against PTP1B and GPa are herein reported.

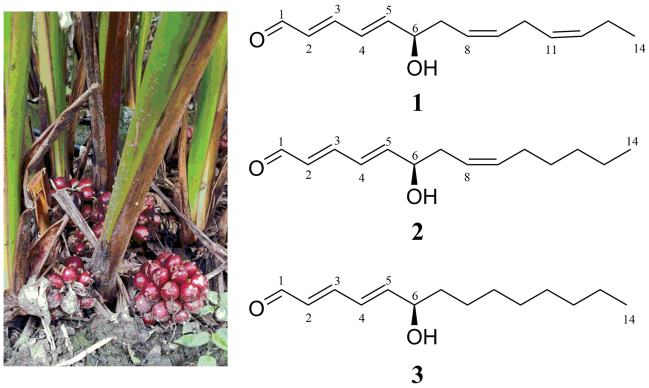

Figure 1: Plants of *A. tsao-ko* and the structures of three new hydroxytetradecenals **1**−**3**

2 Materials and Methods

2.1 General Experimental Procedures

High-resolution mass spectra (HRESIMS) were measured with an LC/MS-IT-TOF spectrometer. Optical rotations were detected by a JASCO P-1020 digital polarimeter. 1D and 2D NMR spectra were measured with an Advance III-600 instrument. Thin-layer chromatography (TLC) analysis was performed on silica

gel plates by spraying with 10% H_2SO_4. A Shimadzu LC-CBM-20 system with an Agilent XDB-C_{18} column was used for high-performance liquid chromatography (HPLC) purification.

2.2 Plant Materials

The fruits of *Amomum tsao-ko* Crevost et Lemarie were collected from Nujiang, Yunnan Province of China in 2022, and were authenticated by Yi Yang (Nujiang Green Spice Industry Research Institute). A voucher specimen (No. 20220701At) was deposited at the State Key Laboratory of Phytochemistry and Plant Resources in West China, Kunming Institute of Botany, Chinese Academy of Sciences.

2.3 Extraction and Isolation

The dried and ground fruits of *A. tsao-ko* (1 kg) were extracted with petroleum ether (PE) at room temperature twice (12 L each). The combined extraction was evaporated under vacuum, and separated through silica gel CC, employing ethyl acetate (EtOAc)-PE system (from 2:98 to 50:50, *v/v*). The EtOAc-PE (5:95, *v/v*) fraction was separated by Sephadex LH-20 CC [methanol (CH_3OH)-chloroform ($CHCl_3$), 50:50, *v/v*] and HPLC [C_{18} column, acetonitrile (CH_3CN)-H_2O (75:25, *v/v*)] to yield **1** (4 mg), **2** (3 mg) and **3** (0.5 mg).

2.4 Spectroscopic Data

(2*E*,4*E*,8*Z*,11*Z*)-6*R*-Hydroxytetradeca-2,4,8,11-tetraenal (**1**):

Pale yellow oil. $[\alpha]_D^{24}$ −5.45 (*c* 0.11, MeOH); ^1H and ^{13}C NMR (DEPT), see data on Table 1; HRESIMS *m/z* 221.1521 Da ($[M + H]^+$, calculated for $C_{14}H_{21}O_2$, 221.1536 Da, −1.5 mDa); UV (MeOH) λ_{max} (log ε): 272 nm.

(2*E*,4*E*,8*Z*)-6*R*-Hydroxytetradeca-2,4,8-trienal (**2**):

Pale yellow oil. $[\alpha]_D^{21}$ −3.78 (*c* 0.09, MeOH); ^1H and ^{13}C NMR (DEPT), see data on Table 1; HRESIMS *m/z* 223.1700 Da ($[M+H]^+$, calculated for $C_{14}H_{23}O_2$, 223.1693 Da, +0.7 mDa); UV (MeOH) λ_{max} (log ε): 273 nm.

(2*E*,4*E*)-6*R*-Hydroxytetradeca-2,4-dienal (**3**):

Pale yellow oil. $[\alpha]_D^{24}$ −6.60 (*c* 0.02, MeOH); ^1H and ^{13}C NMR (DEPT) see data on Table 1; HRESIMS *m/z* 225.1835 Da ($[M+H]^+$, calculated for $C_{14}H_{25}O_2$, 225.1849 Da, −1.4 mDa); UV (MeOH) λ_{max} (log ε): 272 nm.

2.5 Enzyme Inhibition Assays

Enzyme inhibition assays followed the previous method with minor modifications [27,28]. In the PTP1B inhibition assay, 100 mL of working buffer containing 3-(N-morpholino)propanesulfonic acid (MOPS, 722.0 mg), dithiothreitol (DTT, 30.0 mg), ethylene diamine tetraacetic acid (EDTA, 25.7 mg) and NaCl (12.1 g) was prepared before the test. Tested samples (10 μL), working buffer (70 μL), and PTP1B enzyme (10 μL) were pipetted into 96-well plates, followed by an incubation for 15 min. After adding the substrate (10 μL), the mixture was incubated for 30 min. To the mixture, 100 μL of Na_2CO_3 was added, and the absorbance was recorded on a FlexA-200 microplate reader. In the GPa inhibitory assay, tested samples (10 μL) and enzyme (50 μL) were added into 96-well plates, and incubated at 37°C for 15 min. After the addition of substrate solution (40 μL), the mixture was incubated for 30 min. Then, the mixture was supplemented with 150 μL of HCl containing ammonium molybdate (10 mg/mL) and malachite green (0.38 mg/mL). After incubation for 20 min, the absorbance was recorded at 620 nm. Sodium orthovanadate (Na_3VO_4) and CP-91149 were applied as the respective positive controls.

Table 1: ^{1}H and ^{13}C NMR data of compounds **1**–**3** in $CDCl_3$.[a]

No.	1		2		3	
	δ_C	δ_H	δ_C	δ_H	δ_C	δ_H
1	193.9 CH	9.57 1H d (7.9)	193.9 CH	9.57 1H d (7.9)	193.9 CH	9.57 1H d (7.9)
2	132.1 CH	6.17 1H dd (15.3, 7.9)	132.0 CH	6.17 1H dd (15.3, 7.9)	132.0 CH	6.17 1H dd (15.2, 7.9)
3	151.4 CH	7.11 1H dd (15.3, 11.0)	151.5 CH	7.11 1H dd (15.3, 11.0)	151.6 CH	7.11 1H dd (15.2, 10.7)
4	127.7 CH	6.56 1H dd (15.3, 11.0)	127.7 CH	6.58 1H m	127.5 CH	6.51 1H dd (15.3, 10.7)
5	146.4 CH	6.28 1H dd (15.3, 5.5)	146.5 CH	6.28 1H dd (15.3, 5.5)	147.4 CH	6.26 1H dd (15.3, 5.7)
6	71.2 CH	4.36 1H q (5.5)	71.3 CH	4.34 1H q (5.5)	72.1 CH	4.30 1H q (5.5)
7	35.2 CH_2	2.41 2H t-like (6.9)	35.2 CH_2	2.38 2H t-like (6.8)	37.2 CH_2	1.68–1.20 2H overlap.
8	123.8 CH	5.41 1H dt (10.5)	123.4 CH	5.37 1H dt (10.5, 6.8)	25.4 CH_2	1.68–1.20 2H overlap.
9	133.0 CH	5.62 1H dt (10.5, 7.3)	135.1 CH	5.64 1H dt (10.5, 7.0)	29.4 CH_2	1.68–1.20 2H overlap.
10	25.9 CH_2	2.81 2H t (7.3)	27.6 CH_2	2.05 2H q (7.0)	29.6 CH_2	1.68–1.20 2H overlap.
11	126.5 CH	5.29 1H dt (10.5, 7.3)	29.4 CH_2	1.41–1.21 2H overlap.	29.6 CH_2	1.68–1.20 2H overlap.
12	132.6 CH	5.41 1H dt (10.5, 7.4)	31.6 CH_2	1.41–1.21 2H overlap.	32.0 CH_2	1.68–1.20 2H overlap.
13	20.8 CH_2	2.07 2H p (7.4)	22.7 CH_2	1.41–1.21 2H overlap.	22.8 CH_2	1.68–1.20 2H overlap.
14	14.4 CH_3	0.97 3H t (7.4)	14.2 CH_3	0.88 3H t (7.0)	14.3 CH_3	0.88 3H t (6.9)

Note: [a] δ_C and δ_H in ppm mean chemical shifts of carbons and protons; s, d, t, q, p, dd, dt, m mean the split of peaks in ^{1}H NMR spectra; overlap (overlapped); The data of δ_H in parentheses represent the spin-spin coupling constants (J) in Hz.

3 Results and Discussion

3.1 Structure Elucidation

Compound **1** had a molecular formula of $C_{14}H_{20}O_2$ which was assigned by HRESIMS at *m/z* 221.1521 Da ($[M + H]^+$, calculated for $C_{14}H_{21}O_2$, −1.5 mDa), with five degrees of unsaturation. Its ^{13}C NMR (DEPT) data exhibited 14 carbons ascribed to an aldehyde group, eight sp^2 methines, one oxygenated methine, three methylenes, and a methyl. In the ^{1}H NMR spectrum, an aldehyde proton at δ_H 9.57, two *trans*-double bonds at δ_H 6.17 and 7.11 (J = 15.3 Hz) and δ_H 6.56 and 6.28 (J = 15.3 Hz), two *cis*-double bonds at δ_H 5.41 and 5.62 (J = 10.5 Hz) and δ_H 5.29 and 5.41 (J = 10.5 Hz), and a methyl in triplet at δ_H 0.97, were recognized.

The ^{1}H and ^{13}C NMR data of **1** showed high similarity with lycocasuarinen acid E [29], except that a carboxyl group and two *trans*-double bonds in lycocasuarinen acid E were changed to be an aldehyde group and two *cis*-double bonds in **1**. With the aid of the ^{1}H-^{1}H COSY experiment, the consecutive correlations

from H-1 to H-14 established the C_{14} chain. Moreover, the ROESY correlations of H-1 with H-3, H-3 with H-5, and H-2 with H-4 verified the *E*-form of $\Delta^{2,4}$-diene; the correlations of H-7 with H-10, and H-10 with H-13 verified the *Z*-form of $\Delta^{8,11}$-diene (Fig. 2).

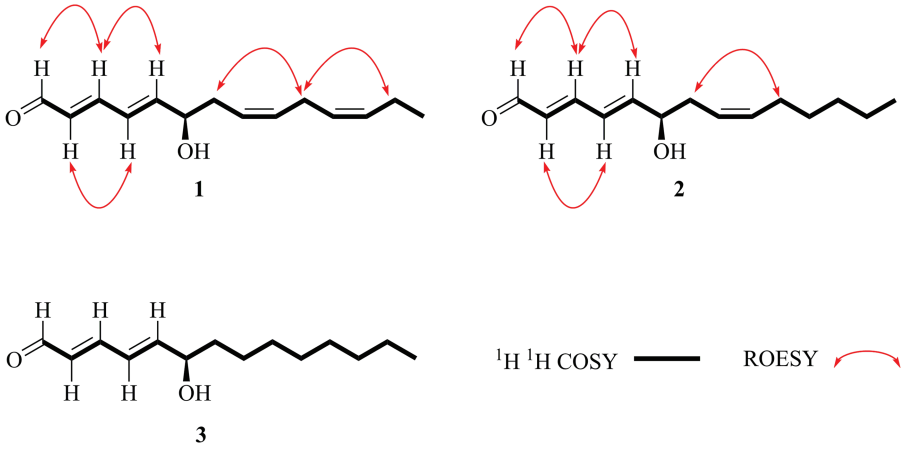

Figure 2: Key 2D NMR correlations of three new hydroxytetradecenals **1**−**3**

The stereochemistry of C-6 was determined to be *R* by its negative rotation ($[\alpha]_D^{24}$ −5.45), opposite to (2*E*,4*E*)-6*S*-hydroxyldodeca-2,4-dienoic acid ($[\alpha]_D^{20}$ +11.7) [29]. Hence, compound **1** was characterized as (2*E*, 4*E*, 8*Z*, 11*Z*)-6*R*-hydroxytetradeca-2,4,8,11-tetraenal (**1**).

Compound **2** was assigned the molecular formula of $C_{14}H_{22}O_2$ according to its HRESIMS at *m/z* 223.1700 Da ($[M+H]^+$, calculated for $C_{14}H_{23}O_2$, +0.7 mDa), showing four degrees of unsaturation. The NMR data of **2** are similar to **1** besides the absence of one *cis*-double bond and two extra methylenes. In the ^{1}H-^{1}H COSY spectrum, the consecutive correlations from H-1 to H-14 verified the $\Delta^{2,4,8}$-triene pattern in the structure. Thus, compound **2** was suggested to be the 11,12-dihydro derivative of **1**. The Δ^2- and Δ^4-double bonds were deduced as *trans*-form by the coupling constant of 15.3 Hz, and the Δ^8-double bond was deduced as *cis*-form by the coupling constant of 10.5 Hz. This deduction was further confirmed by the ROESY correlations of H-1/H-3/H-5, H-2/H-4, and H-7/H-10. Similarly, the configuration of C-6 was assigned to be *R* by the negative rotation (−3.78). Thus, compound **2** was identified as (2*E*,4*E*,8*Z*)-6*R*-hydroxytetradeca-2,4,8-trienal (**2**).

Compound **3** had a molecular formula of $C_{14}H_{24}O_2$ which was deduced from the HRESIMS at *m/z* 225.1835 Da ($[M+H]^+$, calculated for $C_{14}H_{25}O_2$, −1.4 mDa), with two more hydrogens (H) than **2**. Compared with **2**, the ^{1}H and ^{13}C NMR data suggested the presence of two extra methylenes but the absence of one *cis*-double bond. From the above features, compound **3** was proposed to be the 8,9-dihydro derivative of **2**, and was further supported by the ^{1}H-^{1}H COSY correlations from H-1 to H-14. The configuration of $\Delta^{2,4}$-diene was settled as *E* by the coupling constant of 15.2 Hz. Its absolute configuration was determined to be 6*R* by the negative rotation (−6.60). Finally, compound **3** was deduced as (2*E*, 4*E*)-6*R*-hydroxytetradeca-2,4-dienal (**3**).

3.2 Enzyme Inhibitory Activity

PTP1B and GPa are two potential therapeutic targets for the treatment of diabetes. PTP1B as a hydrolase located on the cytoplasmic surface of the endoplasmic reticulum (ER) is widely expressed in insulin-target tissues [30]. By inducing the dephosphorylation of phosphorylated insulin receptor and insulin receptor substrate 1 (IRS1), PTP1B terminates IR signaling and inhibits glucose uptake, thus resulting in insulin resistance [31]. Also, PTP1B can dephosphorylate and inactivate the leptin receptor-associated kinase

JAK-2, thereby blocking the signal transduction of leptin [32]. Glycogen phosphorylase (GP) is the key enzyme in catalyzing the rate-limiting step of glycogen degradation. GPa is the active form of GP, inhibiting which can significantly lower the fasting plasma glucose in type 2 DM patients [33,34]. To assess their hypoglycemic potency, compounds **1** and **2** were tested for the PTP1B and GPa inhibitory activity. In Table 2, compounds **1** and **2** displayed moderate inhibition against PTP1B with inhibition rates of 40.2% ± 1.0%, 50.3% ± 0.6% at 200 μM, and 33.8% ± 1.6%, 41.1% ± 2.6% at 100 μM. For the GPa inhibitory assay, compound **1** exhibited high activity with inhibition rates of 94.8% ± 0.2% (200 μM) and 89.8% ± 2.9% (100 μM), whereas compound **2** was inactive at the tested concentrations. The IC_{50} value of **1** on GPa was calculated as 31.7 μM by a dose-response study (Fig. 3). Compound **3** was not tested for inhibitory activity due to the inadequate amount.

Table 2: PTP1B and GPa inhibitory activity of compounds **1**–**2**.[a]

Compounds	**1**			**2**		
Inhibition (%)	Concentration					
	200 μM	100 μM	IC_{50} (μM)	200 μM	100 μM	IC_{50} (μM)
PTP1B	40.2 ± 1.0	33.8 ± 1.6	/[b]	50.3 ± 0.6	41.1 ± 2.6	195.5
GPa	94.8 ± 0.2	89.8 ± 2.9	31.7	−7.0 ± 1.4	−11.9 ± 2.2	/

Note: [a] Data were presented as mean ± SD ($n = 3$), sodium orthovanadate (Na_3VO_4) (IC_{50} = 194.0 μM) and CP-91149 (IC_{50} = 1.7 μM) were applied as the positive controls. [b] IC_{50} value was not tested.

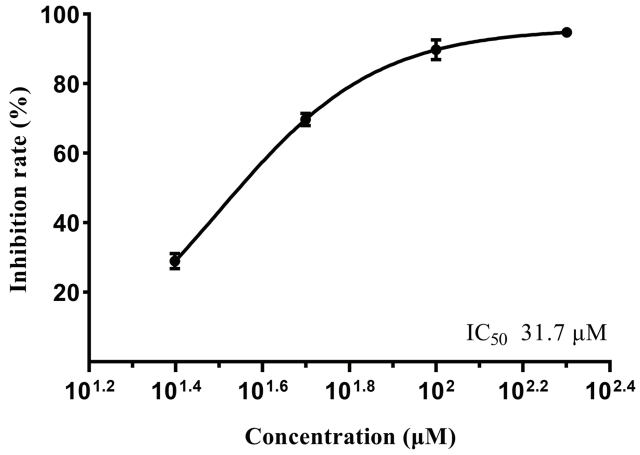

Figure 3: Dose-response curve of compound **1** on GPa

The fruits of *A. tsao-ko* (Cao-Guo) are widely used as both medicinal materials and food additives in China, showing diverse pharmacological activities such as antibiotic, anti-inflammatory, anticancer, antidiabetic, and neuroprotective effects [11]. Previously, the extracts of *A. tsao-ko* were reported to have *α*-amylase and *α*-glucosidase inhibitory activity *in vitro* [35] and hypoglycemic activity *in vivo* [12].

To search for antidiabetic clues from Zingiberaceae plants, our previous study reported a series of flavanol-fatty alcohol hybrids, flavanol-monoterpenoid hybrids, and diarylheptanoids which showed PTP1B and *α*-glucosidase inhibitory activity from the EtOAc part of *A. tsao-ko* [20–24]. Although the low-polarity volatile oils in *A. tsao-ko* had been revealed with antibiotic, cytotoxic, and antioxidant effects, their antidiabetic potency was still unclear [11]. In connection with our previous research, the petroleum ether soluble part was further studied, from which three new hydroxytetradecenals were

obtained and fully determined by HRMS, NMR, and $[\alpha]_D$ data. Their effects against two diabetes-related enzymes PTP1B and GPa were assayed *in vitro*. Two compounds (**1** and **2**) exhibited moderate inhibition on PTP1B, and compound **1** showed obvious inhibition on GPa. This study further enriched the antidiabetic constituents of *A. tsao-ko*.

4 Conclusion

In this study, three new hydroxytetradecenals were isolated from the petroleum ether-soluble part of Cao-Guo. Structurally, compounds **1**−**3** are highly related but with different numbers of double bonds. Both compounds **1** and **2** showed inhibition on PTP1B, but only compound **1** was active to GPa, suggesting that the number of *cis*-double bonds highly influenced the activity. This study demonstrates that the low-polarity hydroxytetradecenals contribute to the antidiabetic potency of Cao-Guo, in addition to the middle-polarity phenols as described in our previous reports. Thus, *A. tsao-ko* could be considered as an alternative herb used alone or in combination for the treatment of diabetes.

Acknowledgement: Not applicable.

Funding Statement: This work was financially supported by the Yunnan Major Scientific and Technological Program (202202AE090035), Xingdian Yingcai Project (YNWR-QNBJ-2018-061), the Yunnan Fundamental Research Projects (202201AV070010, 202301AS070069), Yunnan Province Science and Technology Department (202305AH340005), and the Fund of State Key Laboratory of Phytochemistry and Plant Resources in West China (P2022-KF12).

Author Contributions: Xiaolu Qin carried out the isolation, and structure elucidation, and wrote the manuscript; Xinyu Li, Shengli Wu, and Pianchou Gongpan performed the bioassay and helped with writing; Yi Yang, Mei Huang, Lianzhang Wu, and Juncai He helped to collect the plant materials and provided guidance during the experiment; Changan Geng designed and guided the research and revised the manuscript. All data were generated in-house, and no paper mill was used. All authors agree to be accountable for all aspects of work ensuring integrity and accuracy.

Availability of Data and Materials: The data that support this study will be shared upon reasonable request to the corresponding author.

Ethics Approval: Not applicable.

Conflicts of Interest: The authors declare that they have no conflicts of interest to report regarding the present study.

Supplementary Materials: The supplementary material is available online at https://doi.org/10.32604/phyton.2024.048192.

References

1. Pereira FD, Cazarolli HL, Lavado C, Mengatto V, Figueiredo MSRB, Guedes A, et al. Effects of flavonoids on α-glucosidase activity: potential targets for glucose homeostasis. Nutr. 2011;27(11–12):1161–7. doi:10.1016/j.nut.2011.01.008.
2. Kerru N, Singh-Pillay A, Awolade P, Singh P. Current anti-diabetic agents and their molecular targets: a review. Eur J Med Chem. 2018;152:436–88. doi:10.1016/j.ejmech.2018.04.061.
3. American Diabetes Association Professional Practice Committee. Classification and diagnosis of diabetes: standards of medical care in diabetes—2022. Diabetes Care. 2022;45(Suppl 1):S17–38. doi:10.2337/dc22-S002.
4. DeMarsilis A, Reddy N, Boutari C, Filippaios A, Sternthal E, Niki K, et al. Pharmacotherapy of type 2 diabetes: an update and future directions. Metabolism. 2022;137:155332. doi:10.1016/j.metabol.2022.155332.

5. Ning C, Jiao YH, Wang JQ, Li WW, Zhou JQ, Lee YC, et al. Recent advances in the management of type 2 diabetes mellitus and natural hypoglycemic substances. Food Sci Hum Wellness. 2022;11(5):1121–33. doi:10.1016/j.fshw.2022.04.004.
6. Rasouli H, Yarani R, Pociot F, Popović-Djordjević J. Anti-diabetic potential of plant alkaloids: revisiting current findings and future perspectives. Pharmacol Res. 2020;155:104723. doi:10.1016/j.phrs.2020.104723.
7. El-Nashar HAS, Mostafa NM, El-Shazly M, Eldahshan OA. The role of plant-derived compounds in managing diabetes mellitus: a review of literature from 2014 to 2019. Curr Med Chem. 2021;28:4694–730. doi:10.2174/0929867328999201123194510.
8. Aumeeruddy MZ, Mahomoodally MF. Ethnomedicinal plants for the management of diabetes worldwide: a systematic review. Curr Med Chem. 2021;28:4670–93. doi:10.2174/0929867328666210121123037.
9. Rahman MRT, Lou ZX, Yu FH, Wang P, Wang HX. Anti-quorum sensing and anti-biofilm activity of *Amomum tsaoko* (*Amommum tsao-ko* Crevost et Lemarie) on foodborne pathogens. Saudi J Biol Sci. 2017;24(2):324–30. doi:10.1016/j.sjbs.2015.09.034.
10. Starkenmann C, Mayenzet F, Brauchli R, Wunsche L, Vial C. Structure elucidation of a pungent compound in black cardamom: *Amomum tsao-ko* Crevost et Lemarié (Zingiberaceae). J Agric Food Chem. 2007;55(26):10902–7. doi:10.1021/jf072707b.
11. Yang SY, Xue YF, Chen DJ, Wang ZT. *Amomum tsao-ko* Crevost & Lemarié: a comprehensive review on traditional uses, botany, phytochemistry, and pharmacology. Phytother Res. 2022;21:1487–521. doi:10.1007/s11101-021-09793-x.
12. Fan H, Chen M, Dai T, Deng L, Liu C, Zhou W, et al. Phenolic compounds profile of *Amomum tsaoko* Crevost et Lemaire and their antioxidant and hypoglycemic potential. Food Biosci. 2023;52:102508. doi:10.1016/j.fbio.2023.102508.
13. Yang Y, Yang Y, Yan RW, Zhou GL. Cytotoxic, apoptotic and antioxidant activity of the essential oil of *Amomum tsao-ko*. Bioresour Technol. 2009;101(11):4205–11. doi:10.1016/j.biortech.2009.12.131.
14. Zhang TT, Lu CL, Jiang JG. Neuroprotective and anti-inflammatory effects of diphenylheptanes from the fruits of *Amomum tsaoko*, a Chinese spice. Plant Foods Hum Nutr. 2016;71(4):450–3. doi:10.1007/s11130-016-0570-5.
15. Liao LK, Yang ST, Li RY, Zhou W, Xiao Y, Yuan Y, et al. Anti-inflammatory effect of essential oil from *Amomum tsaoko* Crevost et Lemarie. J Funct Foods. 2022;93:105087. doi:10.1016/j.jff.2022.105087.
16. Dai M, Peng C, Sun FH. Anti-infectious efficacy of essential oil from Caoguo (*Fructus Tsaoko*). J Tradit Chin Med. 2016;36(6):799–804. doi:10.1016/s0254-6272(17)30018-3.
17. Liu JZ, Lyu HC, Fu YJ, Cui Q. *Amomum tsao-ko* essential oil, a novel anti-COVID-19 Omicron spike protein natural products: a computational study. Arab J Chem. 2022;15(7):103916. doi:10.1016/j.arabjc.2022.103916.
18. Yu LQ, Shirain N, Suzuki H. Effects of some Chinese spices on body weights, plasma lipids, lipid peroxides, and glucose, and liver lipids in mice. Food Sci Technol Res. 2007;13(2):155–61. doi:10.3136/fstr.13.155.
19. Yu LQ, Shirain N, Suzuki H, Sugane N, Hosono T, Nakajima Y, et al. The effect of methanol extracts of Tsao-ko (*Amomum tsao-ko* Crevost et Lemaire) on digestive enzyme and antioxidant activity *in vitro*, and plasma lipids and glucose and liver lipids in mice. J Nutr Sci Vitaminol. 2010;56(3):171–6. doi:10.3177/jnsv.56.171.
20. He XF, Zhang XK, Geng CA, Hu J, Zhang XM, Guo YQ, et al. Tsaokopyranols A-M, 2,6-epoxydiarylheptanoids from *Amomum tsao-ko* and their α-glucosidase inhibitory activity. Bioorg Chem. 2020;96:103638. doi:10.1016/j.bioorg.2020.103638.
21. He XF, Wang HM, Geng CA, Hu J, Zhang XM, Guo YQ, et al. Amomutsaokols A-K, diarylheptanoids from *Amomum tsao-ko* and their α-glucosidase inhibitory activity. Phytochemistry. 2020;177:112418. doi:10.1016/j.phytochem.2020.112418.
22. He XF, Chen JJ, Huang XY, Hu J, Zhang XK, Guo YQ, et al. The antidiabetic potency of *Amomum tsao-ko* and its active flavanols, as PTP1B selective and α-glucosidase dual inhibitors. Ind Crops Prod. 2021;160(1):112908. doi:10.1016/j.indcrop.2020.112908.
23. He F, Chen JJ, Li TZ, Hu J, Zhang ZK, Guo YQ, et al. Tsaokols A and B, unusual flavanol-monoterpenoid hybrids as α-glucosidase inhibitors from *Amomum tsao-ko*. Chin Chem Lett. 2021;32:1202–5. doi:10.1016/j.cclet.2020.08.050.

24. He XF, Chen JJ, Li TZ, Zhang XK, Guo YQ, Zhang XM, et al. Nineteen new flavanol-fatty alcohol hybrids with α-glucosidase and PTP1B dual inhibition: one unusual type of antidiabetic constituent from *Amomum tsao-ko*. J Agric Food Chem. 2020;68(41):11434–48. doi:10.1021/acs.jafc.0c04615.
25. Li GD, Lu QW, Wang JJ, Hu QY, Liu PH, Yang YW, et al. Correlation analysis of compounds in essential oil of *Amomum tsaoko* seed and fruit morphological characteristics, geographical conditions, locality of growth. Agronomy. 2021;11(4):1–16. doi:10.3390/agronomy11040744.
26. Yang Y, Yang Y, Yan RW, Zou GL. Cytotoxic, apoptotic and antioxidant activity of the essential oil of *Amomum tsao-ko*. Bioresour Technol. 2021;101(11):4205–11. doi:10.1016/j.biortech.2009.12.131.
27. Zhang CC, Geng CA, Huang XY, Zhang XM, Chen JJ. Antidiabetic stilbenes from peony seeds with PTP1B, α-Glucosidase, and DPPIV inhibitory activities. J Agric Food Chem. 2019;67(24):6765–72. doi:10.1021/acs.jafc.9b01193.
28. He XF, Chen JJ, Li TZ, Hu J, Huang XY, Zhang XY, et al. Diarylheptanoid-flavanone hybrids as multiple-target antidiabetic agents from *Alpinia katsumadai*. Chin J Chem. 2023;39(11):3051–63. doi:10.1002/cjoc.202100469.
29. Liu Y, Yao XC, Li J, Zou ZX, Xi C, Xu KP, et al. New unsaturated fatty acids from the aerial parts of *Lycopodiastrum casuarinoides*. Phytochem Lett. 2021;41:55–60. doi:10.1016/j.phytol.2020.11.004.
30. Sukhbi S, Ajmer GS, Rupanshi G, Sharma N, Chopra B, Dhingra AK, et al. Recent updates on development of protein-tyrosine phosphatase 1B inhibitors for treatment of diabetes, obesity and related disorders. Bioorg Chem. 2022;121:105626. doi:10.1016/j.bioorg.2022.105626.
31. Qian S, Zhang M, He Y, Wang W, Liu S. Recent advances in the development of protein tyrosine phosphatase 1B inhibitors for Type 2 diabetes. Future Med Chem. 2016;8(11):1239–58. doi:10.4155/fmc-2016-0064.
32. Panzhinskiy E, Ren J, Nair S. Pharmacological inhibition of protein tyrosine phosphatase 1B: a promising strategy for the treatment of obesity and type 2 diabetes mellitus. Curr Med Chem. 2013;20(21):2609–25. doi:10.2174/0929867311320210001.
33. Spasov AA, Chepljaeva NI, Vorob'ev ES. Glycogen phosphorylase inhibitors in the regulation of carbohydrate metabolism in type 2 diabetes. Russ J Bioorg Chem. 2016;42:133–42. doi:10.1134/S1068162016020138.
34. Martin WH, Hoover DJ, Armento SJ, Stock IA, McPherson RK, Danley DE, et al. Discovery of a human liver glycogen phosphorylase inhibitor that lowers blood glucose *in vivo*. Proc Natl Acad Sci. 1998;95(4):1776–81. doi:10.1073/pnas.95.4.1776.
35. Hussain SA, Hameed A, Fu J, Xiao H, Liu Q, Song Y. Comparative *in vitro* analysis of anti-diabetic activity of Indo-Pak black cardamom (*Amomum subulatum* Roxb) and Chinese black cardamom (*Amomum tsao-ko* Crevost et Lemaire). Prog Nutr. 2018;20:403–14. doi:10.23751/pn.v20i3.6196.